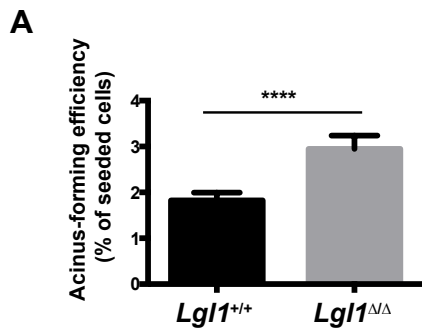


**Cell Reports, Volume 38**

**Supplemental information**

**LGL1 binds to Integrin  $\beta$ 1 and inhibits  
downstream signaling to promote  
epithelial branching in the mammary gland**

**Rongze Ma, Difei Gong, Huanyang You, Chongshen Xu, Yunzhe Lu, Gabriele Bergers, Zena Werb, Ophir D. Klein, Claudia K. Petritsch, and Pengfei Lu**



**Figure S1. *Lgl1* loss does not affect self-renewal using the acinus-forming assay, Related to Figure 1.**

(A) Plot depicting acini-forming efficiency of *Lgl1* het and *Lgl1* KO basal cells. Data points show paired values, and lines indicate mean (n = 4). Statistical analysis was performed using paired t-test and revealed no significant difference between *Lgl1*<sup>+/+</sup> and *Lgl1*<sup>ΔΔ</sup> basal cells. \*\*\*\*, P<0.0001.

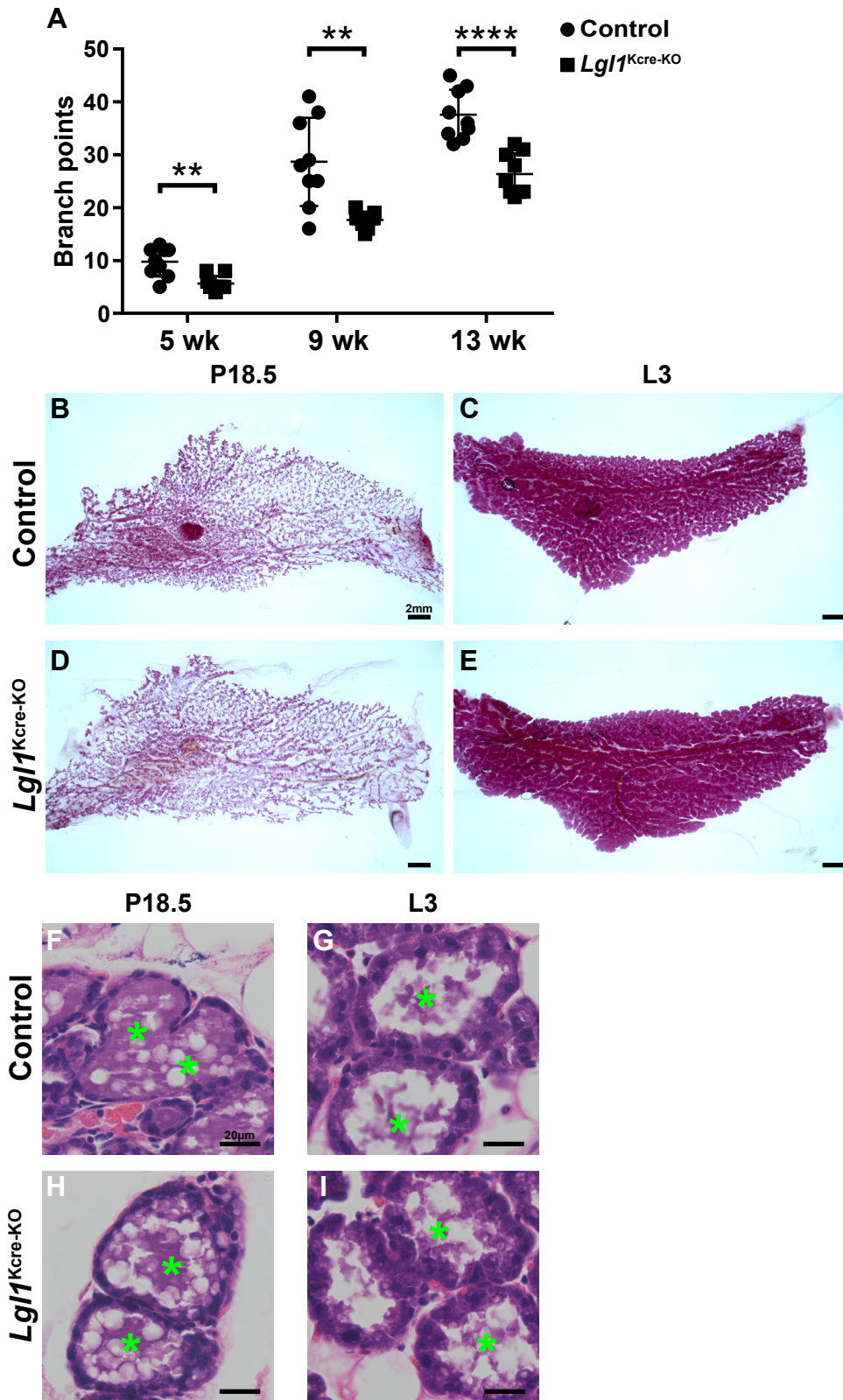


**Figure S2. *Lgl1* promotes branching morphogenesis of the mammary gland epithelium, Related to Figure 2.**

(A) Quantitative comparisons of branching points between control and mutant glands. Plots show mean  $\pm$  SD ( $n \geq 3$ /genotype); \*\*,  $P < 0.01$ ; \*\*\*\*,  $P < 0.0001$ . Scale bars: 2 mm.

(B-F) Mammary epithelium as revealed by Carmine Red staining on wholemount mammary glands of *Lgl1* null and control mice at the stages indicated. Scale bars: 2 mm.

(G-J) Histological analysis by H&E staining of paraffin sections of the mammary glands of *Lgl1* null and control mice at the stages indicated. Green asterisks indicate the milk inside the lumen. Scale bars: 20  $\mu$ m.

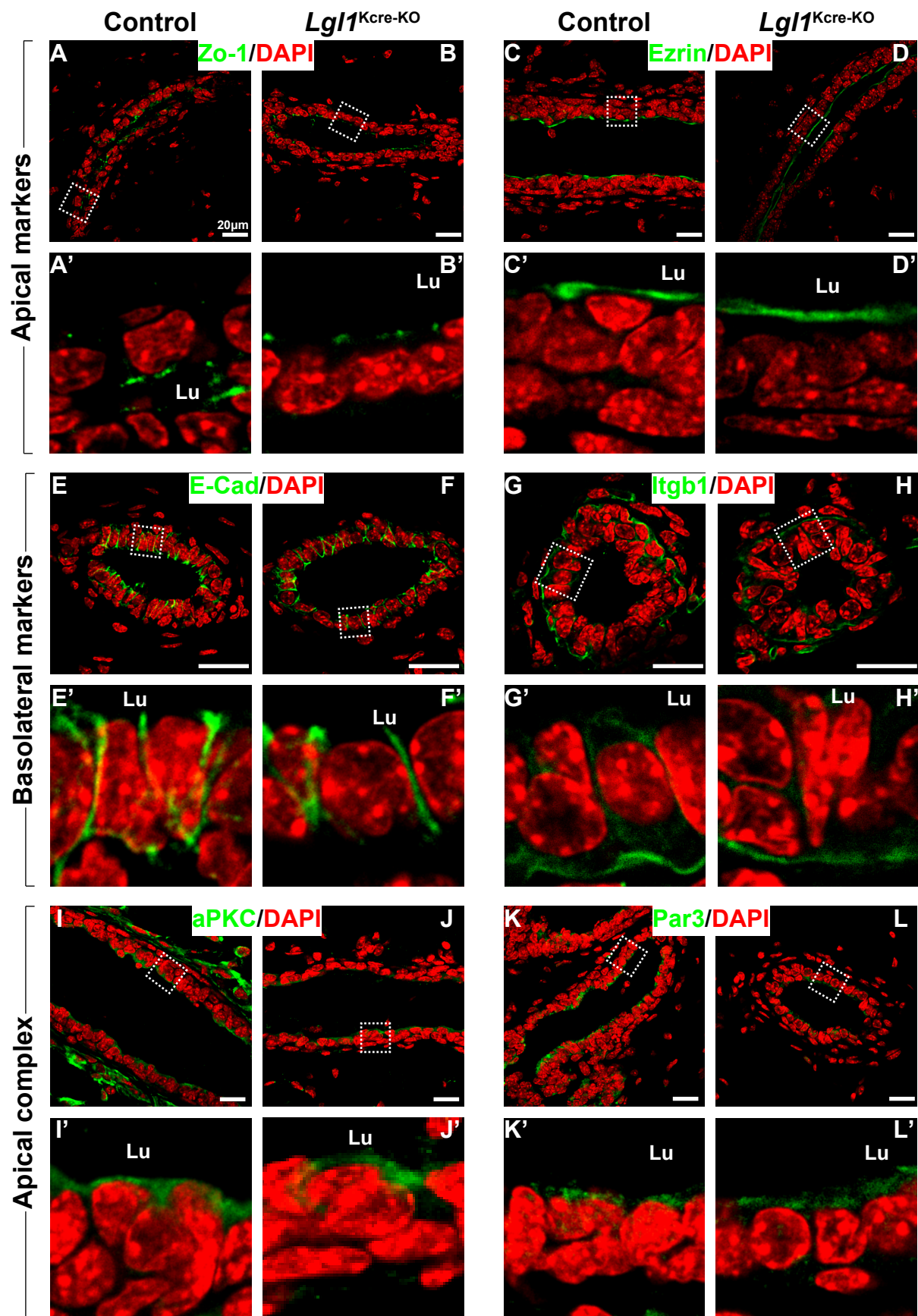


**Figure S3. *Lgl1* is not essential for epithelial polarity in the mammary gland, Related to Figure 3.**

(A-L) Immunofluorescence examination of epithelial apical (A-D) and basolateral polarity markers (E-H) and components of the apical polarity complex (I-L) in 9-wk old mammary glands. Insets are close-up views of an area in the white rectangles with dashed lines. Scale bars: 20 μm.



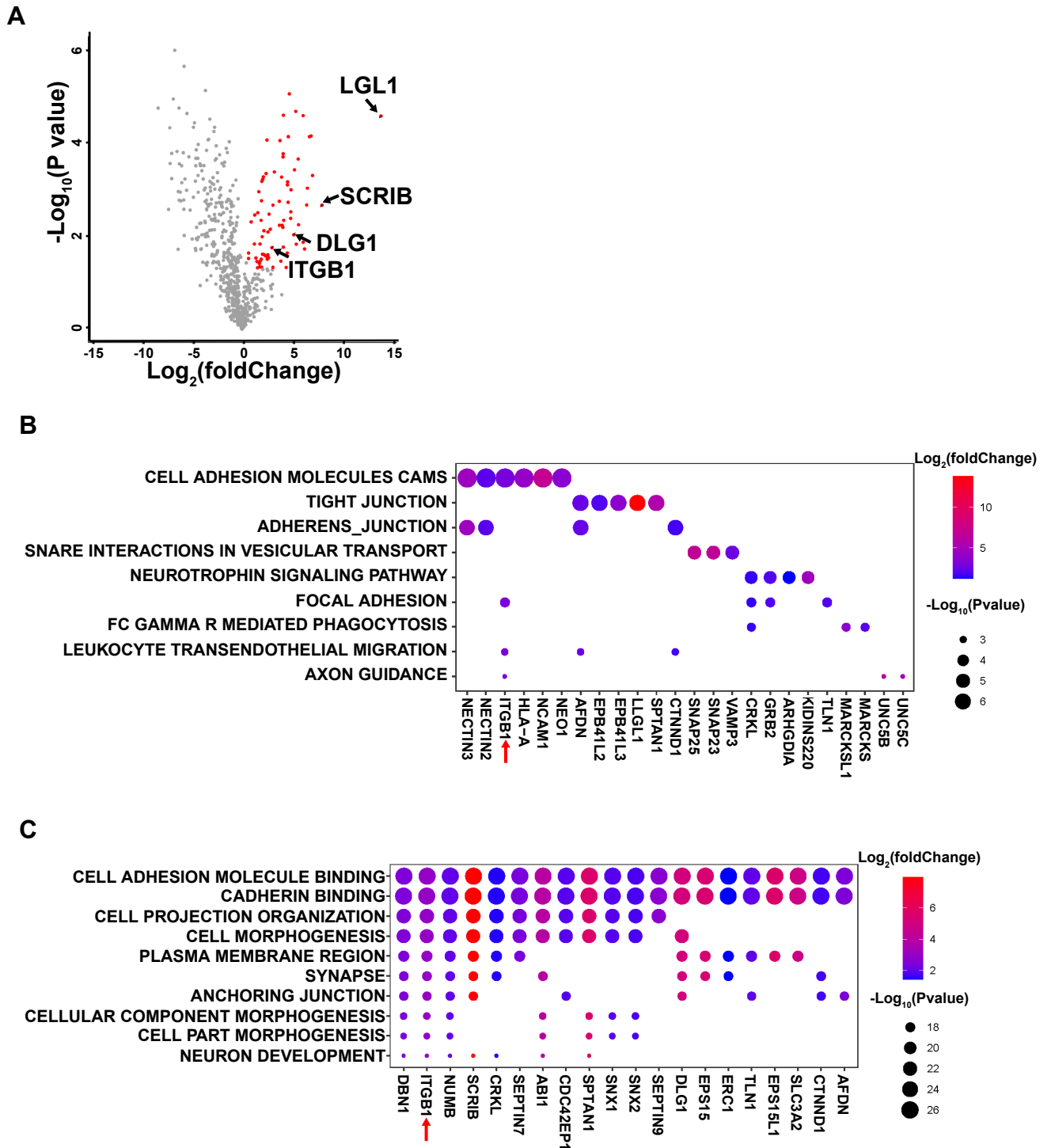


**Figure S4. LGL1 was bound to and co-localized with Integrin, Related to Figure 4.**

(A) Volcano plot showing potential targets from BioID screen. Red arrows indicate known protein partners of LGL1 and ITGB1. (B) Gene Ontology analysis of the differentially ( $P < 0.05$ ) expressed genes with to determine the biological processes (with full description) with which these genes might be involved. (C) KEGG analysis of the differentially ( $P < 0.05$ ) expressed genes to determine the biological processes (with full description) with which these genes might be involved.

A

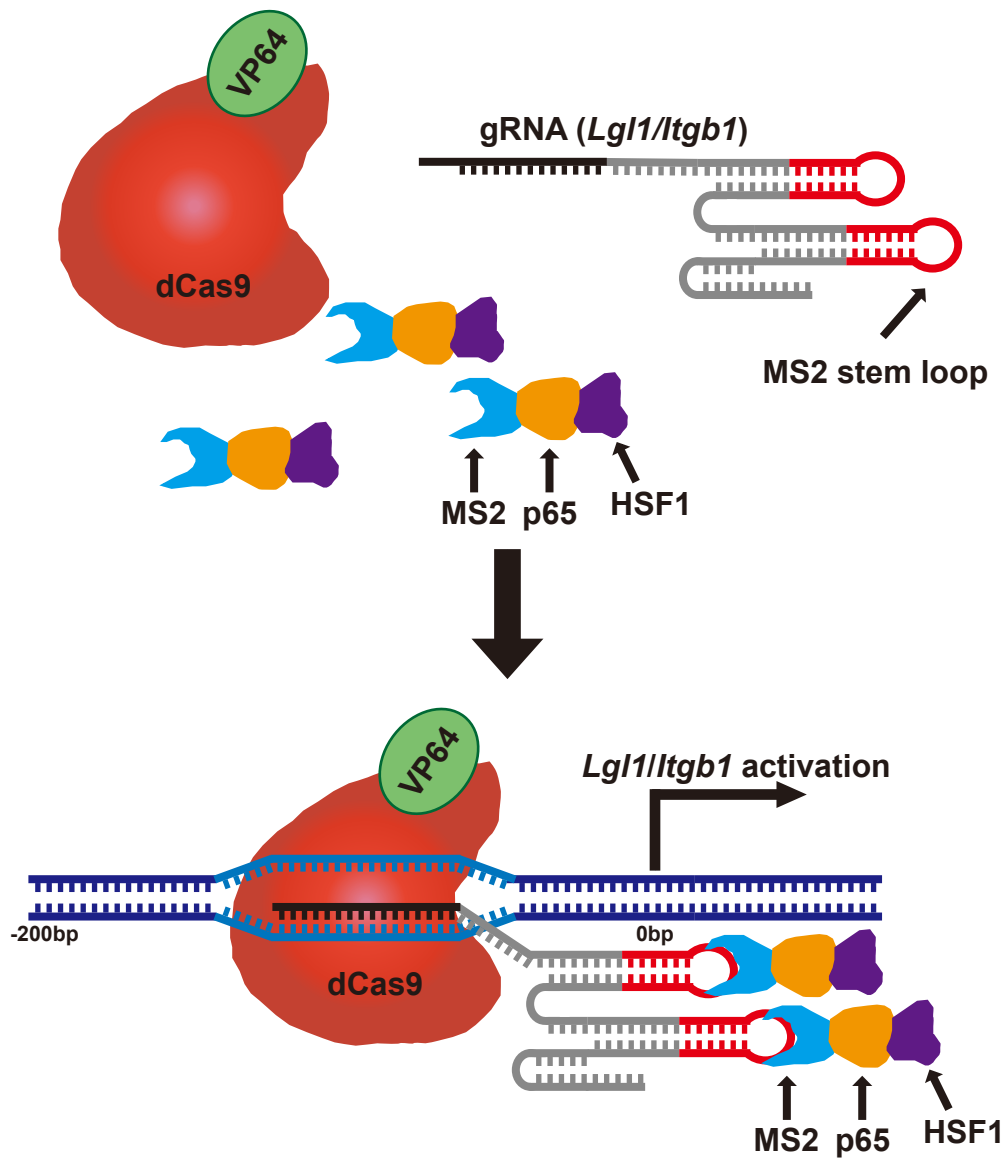


**Figure S5. Overexpression strategy for *Lgl1* and *Itgb1*, Related to Figure 5.**

(A) Gain-of-function of *Lgl1* and *Itgb1* was based on a modified CRISPR technique in which a deactivated Cas9 protein was fused to the transcriptional activator VP64. Target specificity was achieved by using the sgRNA guide sequence from the promoter region of *Lgl1* or *Itgb1*.

Gene name	Forward sequence (5' → 3')	Reverse sequence (5' → 3')
<i>Lgl1</i>	gggtgatgtccacgtcttct	gtgagaagcgcctcaaattcc
<i>Itgb1</i>	atgccaaatcttgccggagaat	ttgctgcgattggtgacatt
<i>Etv4</i>	ccaccaggatcaagaaggaa	ttgtctgggggagtcatagg
<i>Etv5</i>	aggaccccaggctgtacttt	tggccgattcttctggatac
<i>Mkp3</i>	tcgggctgctgctcaagaaac	cggcaaggtcagactcaatgtcc
<i>Actb</i>	ggctgtattcccctccatcg	ccagttggtaacaatgccatgt
<i>Gapdh</i>	ttcaccacatggagaaggc	ccctttggctccaccct

**Table S1. Primers used in qPCR, Related to STAR Methods.**

Total RNA was harvested from mammary glands at the stages indicated. cRNA was prepared as described in Materials and Methods and used as templates for quantitative RT-PCR.

	Pearson's Coefficient	Overlap Coefficient	Manders' Coefficients	
			M1	M2
LGL1 and ITGB1 colocalization	0.55±0.11	0.65±0.09	0.74±0.12	0.29±0.19

**Table S2. Colocalization coefficients of LGL1 and ITGB1, Related to Figure 4.**

Note based on these coefficients, if n=1, it means two proteins have perfect colocalization; whereas if n=0, it means they do not colocalize.